frontiers | Frontiers in Earth Science

TYPE Original Research
PUBLISHED 14 September 2022
DOI 10.3389/feart.2022.1018274

OPEN ACCESS

EDITED BY
Jingshou Liu,
China University of Geosciences
Wuhan, China

REVIEWED BY
Fuhua Shang,
Inner Mongolia University of
Technology, China
Meng Wang,
Chongqing University of Science and
Technology, China

*CORRESPONDENCE
Hu Li,
lihu860628@126.com

SPECIALTY SECTION
This article was submitted to Structural Geology and Tectonics,
a section of the journal
Frontiers in Earth Science

RECEIVED 13 August 2022
ACCEPTED 30 August 2022
PUBLISHED 14 September 2022

CITATION
Li H, Zhou J, Mou X, Guo H, Wang X, An H, Mo Q, Long H, Dang C, Wu J, Zhao S, Wang S, Zhao T and He S (2022), Pore structure and fractal characteristics of the marine shale of the longmaxi formation in the changning area, Southern Sichuan Basin, China. *Front. Earth Sci.* 10:1018274.
doi: 10.3389/feart.2022.1018274

Pore structure and fractal characteristics of the marine shale of the longmaxi formation in the changning area, Southern Sichuan Basin, China

Hu Li[1,2,3,4]*, Jiling Zhou[5], Xingyu Mou[6], Hongxi Guo[6], Xiaoxing Wang[6], Hongyi An[6], Qianwen Mo[6], Hongyu Long[5], Chenxi Dang[7], Jianfa Wu[8], Shengxian Zhao[8], Shilin Wang[2,4], Tianbiao Zhao[2,3,4] and Shun He[2,4]

[1]Shale Gas Evaluation and Exploitation Key Laboratory of Sichuan Province, Chengdu, China, [2]Natural Gas Geology Key Laboratory of Sichuan Province, Chengdu, China, [3]Sichuan College of Architectural Technology, Chengdu, China, [4]School of Geoscience and Technology, Southwest Petroleum University, Chengdu, China, [5]Exploration and Development Research Institute, PetroChina Southwest Oil and Gas Field Company, Chengdu, China, [6]Exploration Division, PetroChina Southwest Oil and Gas Field Company, Chengdu, China, [7]Northwest Sichuan Gas District, PetroChina Southwest Oil and Gas Field Company, Jiangyou, China, [8]Shale Gas Institute, PetroChina Southwest Oil and Gas Field Company, Chengdu, China

The pore structure is an important factor affecting reservoir capacity and shale gas production. The shale reservoir of the Longmaxi Formation in the Changning area, Southern Sichuan Basin, is highly heterogeneous and has a complex pore structure. To quantitatively characterize the shale's pore structure and influencing factors, based on whole rock X-ray diffraction, argon ion polishing electron microscopy observations, and low-temperature nitrogen adsorption-desorption experiments, the characteristics of the shale pore structure are studied by using the Frenkel-Halsey-Hill (FHH) model. The research reveals the following: 1) The pores of the Longmaxi Formation shale mainly include organic pores, intergranular pores, dissolution pores and microfractures. The pore size is mainly micro-mesoporous. Both ink bottle-type pores and semiclosed slit-type pores with good openness exist, but mainly ink bottle-type pores are observed. 2) The pore structure of the Longmaxi Formation shale has self-similarity, conforms to the fractal law, and shows double fractal characteristics. Taking the relative pressure of 0.45 (P/P_0 = 0.45) as the boundary, the surface fractal dimension D_{sf} and the structural fractal dimension D_{st} are defined. D_{sf} is between 2.3215 and 2.6117, and the structural fractal dimension D_{st} is between 2.8424 and 2.9016. The pore structure of micropores and mesopores is more complex. 3) The mineral components and organic matter have obvious control over the fractal dimension of shale, and samples from different wells show certain differences. The fractal dimension has a good positive correlation with the quartz content but an obvious negative correlation with clay minerals. The higher the total organic carbon content is, the higher the degree of thermal evolution, the more complex the pore

structure of shale, and the larger the fractal dimension. The results have guiding significance for the characterization of pore structure of tight rocks.

KEYWORDS

self-similarity, fractal dimension, pore structure, influencing factors, rich in organic shale, longmaxi formation, Changning area

Introduction

Shale gas is a high-quality unconventional natural gas resource under the "carbon peaking and carbon neutralization" policy and has the characteristics of enormous resources, cleanness, and efficiency. Sichuan Basin is a key target area for shale gas exploration and development in China. The marine shale of the Wufeng-Longmaxi Formation has the characteristics of a high TOC value, large thickness, high maturity, good brittleness, and high gas content and is the preferred horizon for shale gas exploration and development (Jin et al., 2018; Fan et al., 2020a, 2020b; Ma et al., 2021; Qiu et al., 2021). Currently, three national shale gas demonstration areas, Fuling, Weiyuan-Changning, and Zhaotong, have been built for the shale gas of the Wufeng-Longmaxi Formation in the Sichuan Basin. These areas mentioned above mainly contain medium-shallow shale gas reservoirs with a buried depth of less than 3,500 m. Organic rich shale generally has the characteristics of low porosity and permeability (porosity less than 8% and permeability less than 10 nD) and mainly develops micron to nanometre pores (He et al., 2021, 2022a; Li et al., 2022a, 2022b; Fan et al., 2022). The pore structure is complex, and the specific surface area is large. The complex internal surface area can store a large amount of gas by adsorption. The proportion of free gas and adsorbed gas in shale is affected by the pore structure of the shale. The more complex the pore structure is, the stronger the adsorption capacity of hydrocarbon gas. The complex pore structure and heterogeneity of shale increase the level of difficulty for shale gas development (Liu J. et al., 2018; Li H. T. et al., 2021, Li et al., 2021 H.; Wang et al., 2021; Zhan et al., 2021). Quantitative characterization of the shale pore structure is of great significance for the effective development of shale gas.

For qualitative or quantitative characterization of the shale pore structure, environmental scanning electron microscopy, argon ion polishing technology, transmission electron microscopy, the mercury intrusion method, and the low-pressure gas adsorption method are mainly used at present. However, because the heterogeneity of the shale pore structure does not conform to the traditional European geometric law, these methods cannot be directly used to characterize the heterogeneity of the pore structure. Fractal geometry theory was proposed by Mandelbrot and can be used to characterize special structures that do not conform to European geometric laws and have certain self-similarity (Mandelbrot, 1978, 1984, 1985). In recent years, it has been widely used in the shale pore structure field (Li et al., 2019a; Liu et al., 2020; Li, 2021; Liu et al., 2021). Pore image data, gas or liquid flow test data (such as nitrogen adsorption and mercury intrusion tests), and NMR data can be used to study the pore fractal characteristics (Yang et al., 2017; Liu J. S. et al., 2018; Tang et al., 2019; Wei et al., 2019). For different types of shale reservoir spaces, researchers have attempted to use different models such as the Frenkel-Halsey-Hill (FHH) model, Newton-Kantorovich (NK) model, and Neimark model to carry out fractal research on the shale pore structures (Ahmad and Mustafa, 2006; Pan et al., 2021; Chang et al., 2022). The FHH model is more suitable for rocks with porous media than other models. Also, the FHH model is the most accurate for rock with microporous - mesoporous. In addition, among the various calculation models, the FHH fractal model is widely used in shale pore structure, which is simple to calculate and has strong applicability (Zhang et al., 2018; Li et al., 2019a; Tang et al., 2022).

The Changning area in the Southern Sichuan Basin is close to the basin's edge. The Longmaxi Formation shale has complex sedimentation and structural evolution, forming a large number of multiscale pore and fracture systems, so the heterogeneity of the reservoir pore structure is strong. Based on scanning electron microscopy (SEM), X-ray diffractometry (XRD), and related geochemical experiments, combined with low-temperature nitrogen adsorption experiments, this study quantitatively characterized the pore structure of the Longmaxi Formation shale in the study area by using the commonly used FHH model and analyzed the main influencing factors of the fractal dimension. The research results have guiding significance for the characterization of the pore structure of marine shale and evaluation of the shale gas reservoir capacity.

Geological setting

The Changning area is located at the southern edge of the Sichuan Basin, and its geographical location is located in the south of Changning County, northeast of Junlian County, west of Gao County, and east of Xuyong County. The structure is located at the end of the southwest extension of the high and steep fold belt in Eastern Sichuan, at the junction of the Southern Sichuan fault fold belt and the Loushan fault fold belt, and adjacent to the Southern Huaying Mountain fault fold belt in the west (Figure 1A). The surface of the study area mainly develops NE, NW, EW, and other multidirectional faults and related folds (Fan et al., 2020b; He et al., 2022b). The long axis of the Changning anticline is WNW-ESE, the NE wing is steep, the SW

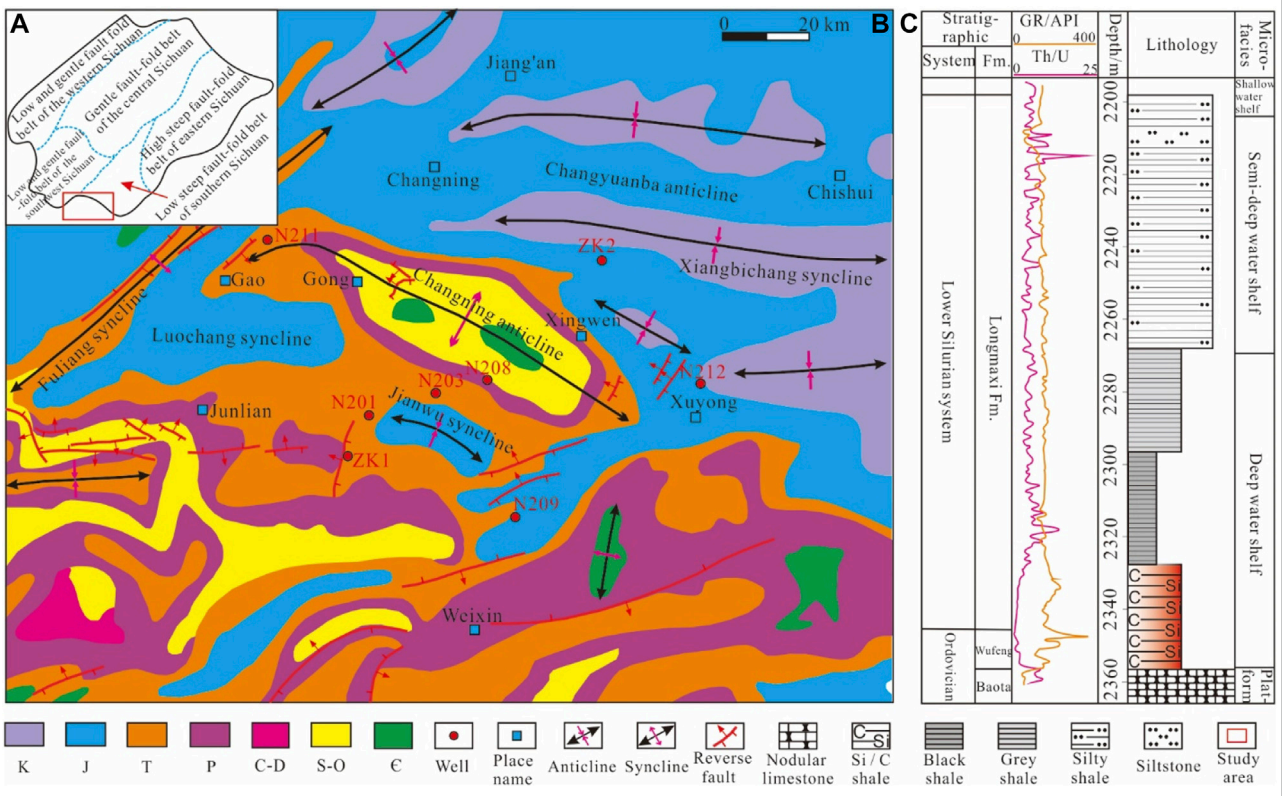

FIGURE 1
Regional geological overview of the Changning area (Wu et al., 2021). **(A)**. Tectonic position (He et al., 2019); **(B)**. Surface geological map; **(C)**. Comprehensive stratigraphic histogram (Feng et al., 2016).

wing is gentle, and the axial plane at the NW end of the anticline is curved, plunging to the south of Gao County, reaching the Jin'e area in the east, and disappearing in the Xuyong syncline. The core of the anticline is exposed to the lower Ordovician, and the two wings of the anticline are exposed to the Silurian, Permian, Triassic, Jurassic, and Cretaceous, along with the Middle Devonian and Carboniferous systems (Figure 1B) (Li et al., 2022c).

From the late Ordovician to the Early Silurian, affected by the Duyun tectonic movement, most areas of the Sichuan Basin were trapped by the subaqueous uplift in Sichuan, the Niushou Mountain-Central Guizhou uplift, and the Jiangnan-Xuefeng uplift, forming a large-scale deep-water depression dominated by the continental shelf. Rapid transgression occurred in the depression, forming a large-scale oxygen-poor/anoxic deep-water shelf environment (Wang et al., 2019). Organic matter and silica are enriched and continuously distributed at the bottom of the Longmaxi Formation, forming an area of 10.7×10^4 km^2 of organic-rich (TOC greater than 2%) cumulative shale facies belt, in which the thickness of the high-quality shale interval is greater than 35 m (Figure 1C).

Samples and methods

Samples and experiments

Due to the influence of weathering, the pore structure of the outcrop samples may change, which cannot reflect the real pore structure characteristics. Therefore, the shale samples were taken from 12 Longmaxi Formation drilling cores from two evaluation wells (ZK_1 and ZK_2) in the study area, and the sampling depth covered Member one of the Longmaxi Formation from bottom to top. The lithology of the sample was mainly black and greyish black organic-rich shale, and the type of organic kerogen was mainly type I and a small amount of type II_1.

The experimental test included organic carbon content (TOC), vitrinite reflectance (Ro), whole rock X-ray diffraction analysis, scanning electron microscopy observations, and low-temperature nitrogen adsorption-desorption experiments. These tests were mainly conducted at the State Key Laboratory of Oil and Gas Reservoir Geology and Development Engineering, and some data were obtained from the Shale Gas Research Institute of PetroChina Southwest Oil and Gas Field Company. The organic carbon content of shale was tested by a CS230SH carbon and

sulfur analyzer produced by Leco company located in the United States, using the solid-state infrared absorption method and following the Standard for the Determination of Total Organic Carbon in Sedimentary Rocks (GB/T 19145-2003). The mineral composition of the whole rock was analyzed according to the SY/T5163-2010 standard and determined by an X'Pert MPD PRO X-ray diffractometer produced by Panaco company in the Netherlands. A Quanta 450 environmental scanning electron microscope made by FEI Company in the United States was used for the Argon ion polishing scanning electron microscopy observations. The working voltage of the instrument was set to 15 kV and 15 nA, and the maximum pore resolution was 3 nm. According to the GB/T16594-2008 standard, an Ilion II 697 argon ion polishing instrument and a Merlin Compact field emission scanning electron microscope were used to determine.

A six-station automatic specific surface area and porosity analyzer (Quantachrome Instruments, United States) was used for the low-temperature nitrogen adsorption experiments. The measured pore size range was 0.35–500 nm. Before the experiment, the samples were placed in deionized water for ultrasonic cleaning to remove surface impurities, and the samples were dried and pretreated after decontamination. Then, the dried samples were manually ground to 20–50 mesh in an agate mortar, and the ground powder samples were vacuum dried for 14 h under a high temperature of 120°C. During the experiment, liquid nitrogen with a purity greater than 99.999% was used as the adsorption medium. Under a constant temperature liquid nitrogen condition of 77 K, the gas adsorption capacity under the gradual increase in the relative pressure and the desorption capacity when the pressure decreased were measured to obtain the isothermal adsorption and desorption data for the sample.

Calculation of the fractal dimension based on nitrogen adsorption and desorption data

According to the International Union of Pure and Applied Chemistry (IUPAC) classification standard of pore size, the pores of shale can be divided into micropores (<2 nm) and mesopores (2–50 nm), and macropores (>50 nm) (Li et al., 2019a; Yang et al., 2022). Organic-rich shale mainly develops micron to nanometre pores, and pores with a diameter of 2–50 nm are the main contributors to shale porosity and the main space for gas enrichment. Research has revealed that the low-temperature liquid nitrogen adsorption-desorption method can better characterize micropores (<2 nm) and mesopores (2–50 nm). Therefore, this study mainly analyses the fractal characteristics of these two types of pores. The fractal dimension of shale is calculated based on the low-temperature nitrogen adsorption curve data for the sample, and the commonly used FHH model is applied:

$$\ln V = K \ln[\ln(P_0/P)] + C \quad (1)$$

$$D = K + 3 \quad (2)$$

$$D = 3K + 3 \quad (3)$$

Where V is the volume of adsorbed gas under different relative pressures, cm^3/g; P_0 refers to the saturated steam pressure, MPa; K is the slope of the equation fitting curve; C is a constant; and D is the fractal dimension.

Different publicity calculations are used to calculate the fractal dimension according to the morphological characteristics of the low-temperature nitrogen adsorption curve. If the surface tension of liquid/gas is the more important factor, the capillary force tends to reduce the interface area, and the fractal dimension is calculated by Formula (2). Suppose the van der Waals force between the solid and the adsorption layer is the main factor, and the adsorption is mainly affected by the surface roughness of the gas/adsorption layer interface. In that case, Formula (3) is used to calculate the fractal dimension. When quantifying the complexity of shale pores, the fractal dimension is between 2 and 3. The larger the fractal dimension is, the more complex the shale pore structure. The object does not have fractal characteristics if the fractal dimension is less than 2 or greater than 3 (Tang et al., 2022).

Results

Pore types and characteristics of shale

Generally speaking, the pores of organic-rich shale mainly include three types: inorganic pores, organic pores, and microfractures. These three types of pores are developed in the Longmaxi Formation shale in the Changning area. Shale has a complex mineral composition and various inorganic pores, including intergranular pores, intragranular pores, intercrystalline pores, and dissolution pores (Wang et al., 2018; Li et al., 2020; Wang and Wang, 2021). Shale has a high degree of the thermal evolution of organic matter, and primary organic pores and hydrocarbon generation shrinkage pores are widely developed. Due to the extrusion of mineral particles and the action of tectonic stress, mineral edge fractures and tectonic microfractures are developed.

Intergranular pores are mostly residual primary pores, the residual intergranular pore space after compaction and water loss transformation in diagenesis (Wang et al., 2020). This type of pore is similar to the residual primary intergranular pores of conventional reservoirs and usually shrinks with the increase in burial depth. Quartz and feldspar minerals are highly brittle, and mineral particles support each other, often forming mineral

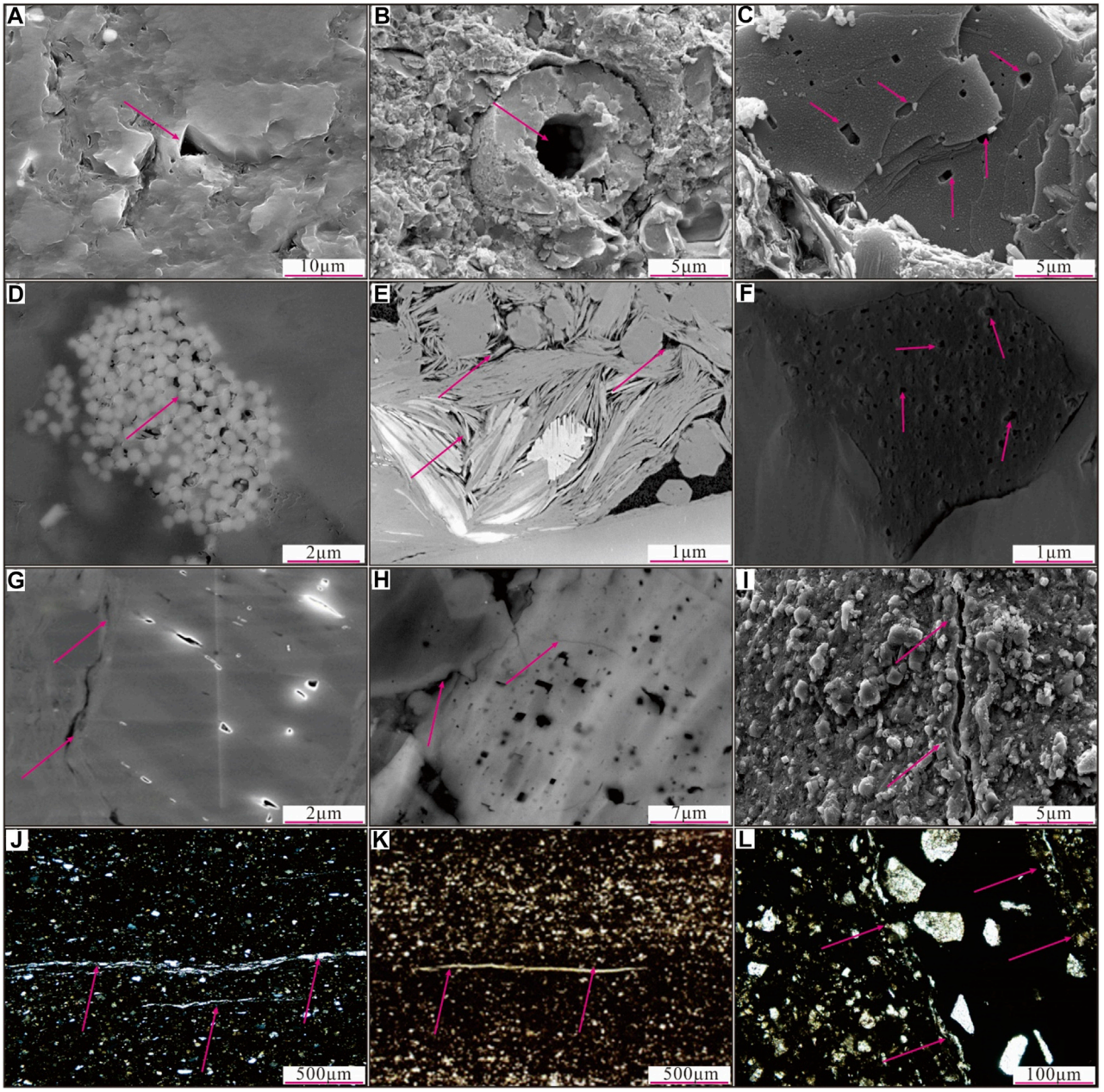

FIGURE 2
Microscopic pore types and characteristics of the Longmaxi Formation shale in the Changning area. **(A)** N216, 2,302.5 m, clay mineral particles supporting residual pores; **(B)** N216, 2,316.7 m, biological cavities developed inside biological particles; **(C)**. ZK_2, 2,233.8 m, intragranular dissolution pores; **(D)**. ZK_2, 233.95 m, intracrystalline pores of strawberry pyrite; **(E)**. N216, 2,308.2 m, intracrystalline pores developed between the crystals of clay minerals; **(F)**. ZK_2, 2,214.37 m, organic pores with a honeycomb distribution; **(G)**. N201, intracrystalline fracture; **(H)**. N216, fracture in the crystal; **(I)**. N216, diagenetic contraction fracture; **(J)**. N216, bedding fracture; **(K)**. N216, hydrocarbon expulsion contraction fracture; **(L)**. N216, dissolution fracture.

intergranular pores, which are mainly produced in a slit or irregular shape (Figure 2A). Intragranular pores are developed in the interior of clastic particles, such as biological cavity pores (Figure 2B) and wall pores of organisms developed in biological particles, and intragranular pores developed in quartz, feldspar, clay, and other particles, some of which form intragranular dissolved pores under the action of an acidic fluid (Figure 2C). Intercrystallite pores are micropores formed by mineral crystallization under the condition of a stable environment and appropriate medium conditions, including

TABLE 1 Mineral composition and vertical changes in the Wufeng-Longmaxi Formation shale in the Changning area.

Well	Sample	Depth (m)	Quartz (%)	Potash feldspar (%)	Plagioclase (%)	Calcite (%)	Dolomite (%)	Pyrite	Clay minerals (%)	TOC (%)	Ro (%)
ZK1	ZK1-1	2,393.51	23.8	1	4.5	26.1	5.5	1.1	38	0.89	2.24
	ZK1-2	2,467.35	35.4	2.5	12.3	8.1	3.3	1.5	36.9	1.56	2.52
	ZK1-3	2,473.58	31	2.3	17.6	11.4	2.7	1.4	33.6	1.11	2.5
	ZK1-4	2,487.10	37.4	1	4.8	12.4	1.9	2.4	40.1	2.1	2.53
	ZK1-5	2,496.31	39.8	1.6	5.2	9.5	4	2.7	37.2	4.89	2.62
	ZK1-6	2,499.29	30.8	0.2	4.1	17.2	12.1	6.4	29.2	4.05	2.48
ZK2	ZK2-1	2,235.60	52.00	1.18	3.78	11.96	18.90	0.95	11.23	4.08	2.75
	ZK2-2	2,223.80	58.88	0.76	3.07	4.90	12.90	1.4	18.10	3.87	2.78
	ZK2-3	2,221.25	49.58	1.32	6.08	9.94	8.80	0.97	23.30	4.13	2.69
	ZK2-4	2,209.20	36.57	1.01	5.75	5.15	2.20	1.02	48.30	2.30	2.65
	ZK2-5	2,188.55	33.22	2.71	9.20	9.09	3.10	0.99	41.70	1.59	2.54
	ZK2-6	2,160.80	27.35	2.79	13.94	10.27	3.40	0.04	42.20	1.19	2.46

pyrite, clay minerals, dolomite, etc., and the pore diameters are mostly distributed between 10 and 500 nm. The most common intercrystallite pores in the study area are strawberry pyrite (Figure 2D) formed in the deep water and anoxic reduction environment and pores developed between the crystals of clay minerals (Figure 2E). The study area mainly develops intergranular organic pores and pyrite-associated organic pores, mainly micropores and mesopores, which contribute greatly to the specific surface area and pore volume of shale and are the main reservoir space of adsorbed natural gas. The content of clastic particles is high, and organic matter fills between the clastic particles and forms organic pores (Figure 2F), which are mainly round and oval.

In addition, the fractures in the study area are widely developed, mainly including three types of microfractures (Wu et al., 2021): 1) mineral intracrystalline fractures and intragranular fractures formed by tectonic action, in which the intracrystalline fractures are also called mineral crystal edge fractures or paste grain fractures (Li et al., 2019a; 2019b). Mineral crystals are deformed and displaced to varying degrees by early tectonic action, forming a certain degree of fractures with the surrounding, and the fracture surfaces are mostly crystal surfaces. The fracture shape coordinates with the crystal boundary, and the opening is approximately 0.01–0.10 μm (Figure 2G). Intragranular fractures, also known as mineral joint fractures, are caused by lattice dislocation or fracture in the crystal under tectonic action (Figure 2H) (Ameen, 2016; Cheng et al., 2021; Shan et al., 2021; Song et al., 2021; Liu et al., 2022a; Wang et al., 2022). 2) Diagenetic contraction fractures and bedding fractures are formed by diagenesis, in which diagenetic contraction fractures are formed by a series of physical and chemical actions such as dehydration, contraction, dry cracking, phase transformation, or recrystallization of sediments during diagenesis, which is characterized by a long extension distance and large opening variation range (Figure 2I). The most prominent feature of bedding fractures is that they are oriented with clay minerals and other minerals, and the opening of fractures can be large or small locally, with a width of approximately 0.01–23.3 μm, which is mostly filled with minerals (Figure 2J). 3) Abnormal high-pressure fractures, hydrocarbon expulsion contraction fractures, and dissolution fractures formed by hydrocarbon generation and expulsion of organic matter, in which abnormal high-pressure fractures are generally developed in shale rich in organic matter, which is mostly controlled by the morphology of kerogen and mineral crystals. Kerogen as the centre extends radially along the surface of the mineral particles and is considered the main transportation channel for the lateral migration of oil and gas. Hydrocarbon expulsion contraction fractures are mainly developed from the interior of organic matter to the edge of organic matter and mineral particles (Gao, 2019; Fan et al., 2020c; Li, 2022). For long-axis organic matter, contraction fractures divide it into multiple sections, most of which are arc-shaped, and the width of the fracture is up to 20 μm in the middle of the fracture arc (Figure 2K). The fracture can also show a slender "hair" shape, bending and pinching out at the end, formed by the volume contraction caused by the dehydration of organic matter at the later stage (Figure 2L) (Ambrose et al., 2010; Li et al., 2018, 2019c).

Mineral composition and organic geochemical characteristics

According to the experimental test data for 12 samples from the two evaluation wells, ZK_1 and ZK_2, in the study area, the shale

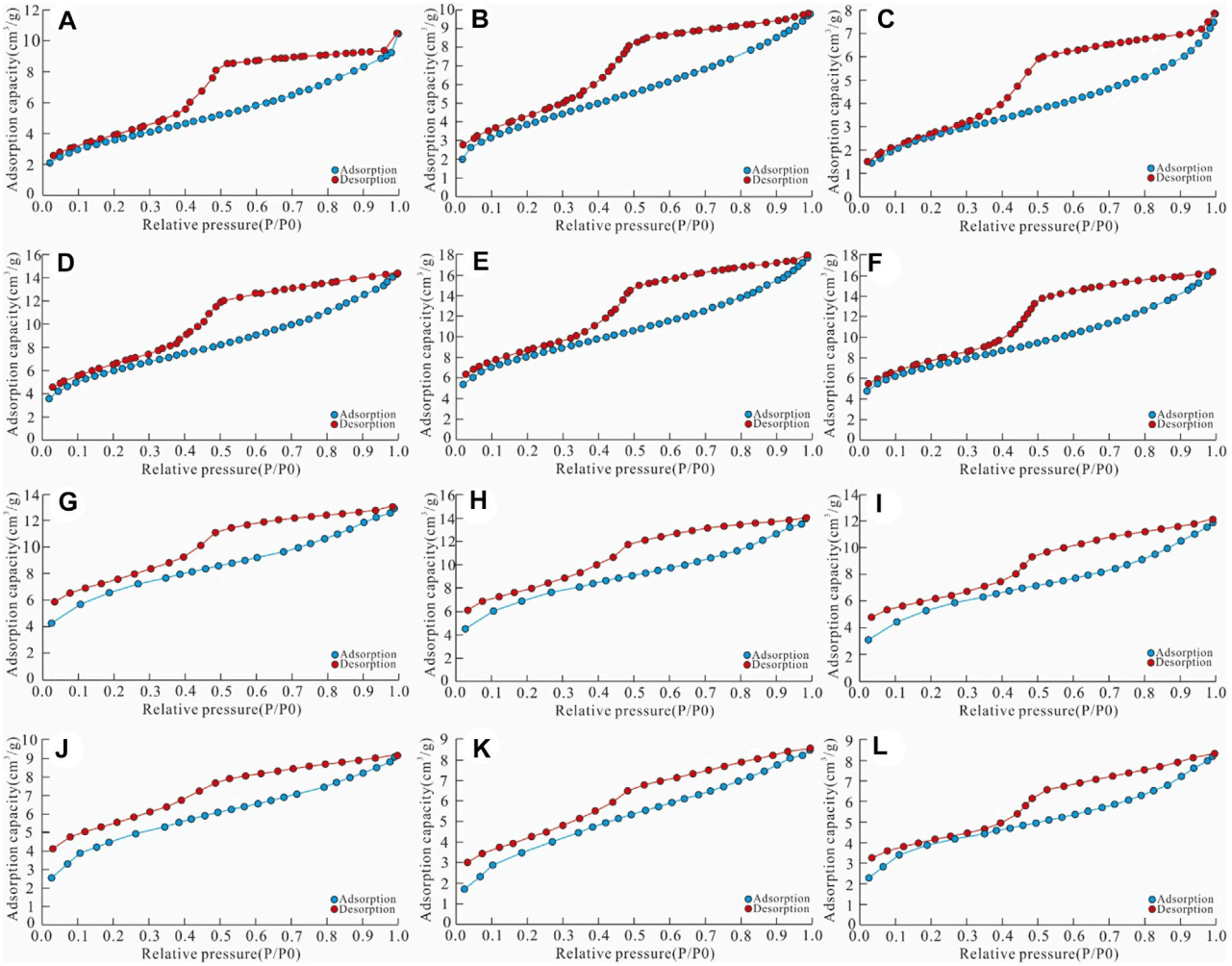

FIGURE 3
Low-temperature nitrogen adsorption-desorption curves of the Longmaxi Formation shale in the Changning area. **(A–F)** is from ZK_1, and **(G–L)** is from ZK_2.

mineral components mainly include quartz, feldspar (potassium feldspar and plagioclase), calcite, dolomite, pyrite, clay minerals, etc. The quartz content of well ZK_1 is between 23.8 and 39.8%, with an average of 33.03%, and that of well ZK_2 is between 27.35 and 58.88%, with an average of 42.93%. The feldspar content of well ZK_1 is between 4.3 and 19.9%, with an average of 9.52%, and that of well ZK_2 is between 3.83 and 16.73%, with an average of 8.60%. The content of carbonate minerals (calcite and dolomite) in well ZK_1 is between 11.4 and 31.6%, with an average of 19.03%, and that in well ZK_2 is between 7.35 and 30.86%, with an average of 16.77%. The clay minerals include mainly illite, along with illite/montmorillonite mixed layer and chlorite. The content of well ZK_1 is between 29.2 and 40.1%, with an average of 35.83%, and that of well ZK_2 is between 11.23 and 48.30%, with an average of 30.81% (Table 1). According to the organic sulfur carbon test results, the TOC and Ro in the study area are both high. The TOC of well ZK_1 is between 0.89 and 4.89%, with an average of 2.43%, and the Ro is between 2.24 and 2.62%, with an average of 2.48%. The TOC of well ZK_2 is between 1.19 and 4.13%, with an average of 2.86%, and the Ro is between 2.46 and 2.78%, with an average of 2.65% (Table 1). Overall, with the increase in depth, the content of quartz and brittle minerals gradually increases, while the content of clay minerals gradually decreases. The content of brittle minerals reaches the maximum at the bottom of the Longmaxi Formation. In addition, the maximum values of TOC and Ro are also at the bottom of the Longmaxi Formation. Due to the different structural positions of the two wells, there are large differences in the mineral components, but the variation rules are the same.

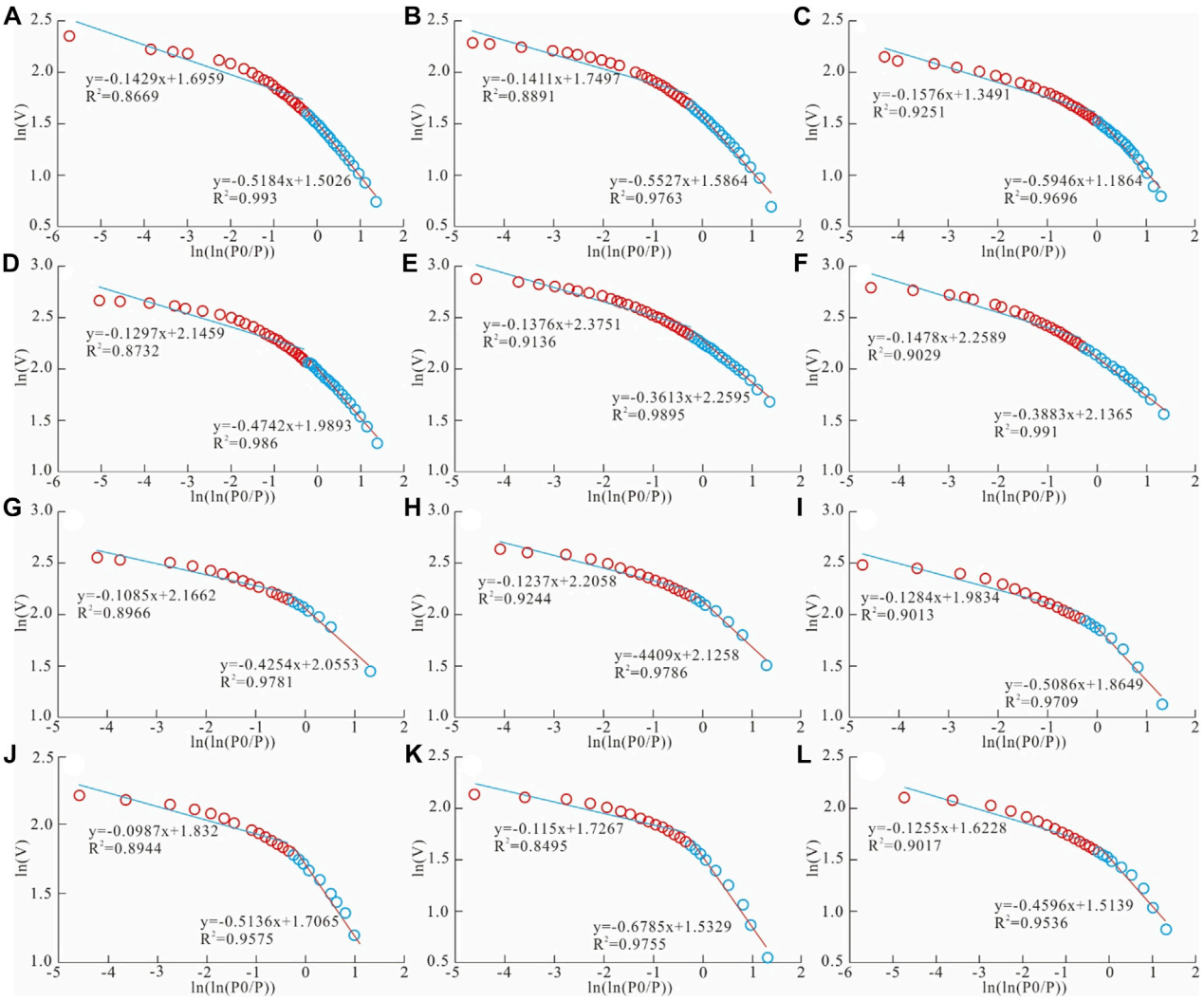

FIGURE 4
ln (V) vs ln [ln (P_0/P)] curves of the Longmaxi Formation shale in the Changning area. **(A–F)** is from ZK_1, and **(G–L)** is from ZK_2.

Pore morphological characteristics

Low-temperature nitrogen adsorption-desorption experiments were carried out on the 12 samples from the two wells in the study area. With the increase in relative pressure, nitrogen was gradually adsorbed on the pore surface of shale, and capillary condensation occurred (Li et al., 2015; Ma et al., 2022). After reaching the maximum pressure, the pressure began to decrease, and the nitrogen adsorbed on the pore surface of shale gradually began to evaporate in the capillary, resulting in desorption. Because the phenomenon of nitrogen desorption is obviously later than that of adsorption at the same pressure, a hysteresis loop is formed (Xu et al., 2017). According to the IUPAC classification of isothermal adsorption curves and hysteresis loops, pores can be divided into four different categories, i.e., cylindrical pores, ink bottle pores, parallel plate pores, and slit pores.

From the low-temperature nitrogen adsorption-desorption curves of the 12 samples (Figure 3). In the relatively low-pressure stage (P/P_0<0.45), the shapes of the adsorption curve and desorption curve are the same, but the two do not coincide. The curve rises slowly and presents an upward slightly convex shape. This stage is the transition from adsorption monolayer to multi-molecular layer. In the relatively high-pressure stage (P/P_0>0.45), the adsorption capacity increases slowly with the increase of pressure, and this stage is a multi-layer adsorption process, the adsorption curve shows obvious hysteresis. According to the shape of the nitrogen adsorption-desorption curve, we believe that the pore morphology in the study area is of two types: mainly ink bottle-type pores along with semiclosed

TABLE 2 Fractal dimension of the Wufeng-Longmaxi Formation shale based on the FHH theoretical model.

Well	Sample	P/Po < 0.45			P/Po > 0.45		
		Fractal fitting equation	R^2	D_1	Fractal fitting equation	R^2	D_2
ZK1	ZK1-1	y = −0.5184x + 1.5026	R^2 = 0.993	2.4816	y = −0.1429x + 1.6959	R^2 = 0.8669	2.8571
	ZK1−2	y = −0.5527x + 1.5864	R^2 = 0.9763	2.4473	y = −0.1411x + 1.7497	R^2 = 0.8891	2.8589
	ZK1-3	y = −0.5946x + 1.1864	R^2 = 0.9696	2.4054	y = −0.1576x + 1.3491	R^2 = 0.9251	2.8424
	ZK1-4	y = −0.4742x + 1.9893	R^2 = 0.9860	2.5258	y = −0.1297x + 2.1495	R^2 = 0.8732	2.8703
	ZK1-5	y = −0.3913x + 2.2595	R^2 = 0.9895	2.6087	y = −0.1376x + 2.3751	R^2 = 0.9136	2.8624
	ZK1-6	y = −0.3883x + 2.1365	R^2 = 0.9910	2.6117	y = −0.1478x + 2.2589	R^2 = 0.9029	2.8522
ZK2	ZK2-1	y = −0.4254x + 2.0553	R^2 = 0.9781	2.5746	y = −0.1085x + 2.1662	R^2 = 0.8966	2.8915
	ZK2-2	y = −0.4409x + 2.1258	R^2 = 0.9786	2.5591	y = −0.1237x + 2.2058	R^2 = 0.9244	2.8763
	ZK2-3	y = −0.5086x + 1.8649	R^2 = 0.9709	2.4914	y = −0.1284x + 1.9834	R^2 = 0.9013	2.8716
	ZK2-4	y = −0.5136x + 1.7065	R^2 = 0.9575	2.4864	y = −0.0987x + 1.8320	R^2 = 0.8944	2.9013
	ZK2-5	y = −0.6785x + 1.5329	R^2 = 0.9755	2.3215	y = −0.1115x + 1.7267	R^2 = 0.8495	2.8885
	ZK2-6	y = −0.4596x + 1.5139	R^2 = 0.9536	2.5404	y = −0.1255x + 1.6228	R^2 = 0.9017	2.8745

slit-type pores with good openness, indicating that micropores, mesopores, and macropores are developed in the shale, but mainly micropores and mesopores occur, which is also why this study only uses low-temperature nitrogen adsorption experiments. Compared with previous studies, there is a big difference in the stage of the high-pressure ratio (Bu et al., 2015; Xi et al., 2018; Liu et al., 2019). We think there may be the following two reasons: first, there are maybe certain errors in the experimental results, but considering the uniqueness of the rocks, we still use these data; the second is that the high-pressure section is mainly filled with macropores, and the proportion of macropores in Longmaxi formation shale in Changning area is small (mainly microporous and mesoporous). Therefore, in the relatively high-pressure stage, the amount of nitrogen filled in the macropores is small, and there will be no sudden increase.

Pore fractal dimension

As mentioned above, when P/P_0 = 0.45, most samples' adsorption and desorption curves begin to become inconsistent. Therefore, we take the relative pressure of 0.45 as the boundary, divide the curve into a "relatively low-pressure section curve" and a "relatively high-pressure section curve", and calculate the fractal dimension of each section. In the relatively low-pressure stage (P/P_0<0.45), the fractal dimension mainly reflects the single molecule and multiple molecule adsorption and filling in the pores, which can be used to indicate the irregularity, roughness, and complexity of the pore surface or can also be used to indicate the complexity of the relatively large pores (mesopores), which we define as the surface fractal dimension D_{sf}. In the relatively high-pressure stage (P/P_0>0.45), gas capillary condensation occurs with increased gas pressure. The fractal dimension usually indicates the complexity of the pore space and structural irregularity, or it can also be used to indicate the complexity of the relative micropores. We define this as the structural fractal dimension D_{st}. Formula (1) is used to create the correlation diagram of ln (V) and ln [ln (P_0/P)] (Figure 4), and linear fitting for different relative pressure sections is conducted. Then, the fractal dimension of the sample pores in the relatively low-pressure and relatively high-pressure stages is calculated through Formula (2). The results show that the surface fractal dimension D_{sf} of well ZK_1 is between 2.4054 and 2.6117, and the structural fractal dimension D_{st} is between 2.8424 and 2.8703. The surface fractal dimension D_{sf} of well ZK_1 is between 2.3215 and 2.5746, and the structural fractal dimension D_{st} is between 2.8716 and 2.9013 (Table 2). Overall, the fractal dimension of the shale pore structure of the Wufeng-Longmaxi Formation in the study area is large, indicating that the shale pore structure is relatively complex. At the same time, the structural fractal dimension D_{st} is greater than the surface fractal dimension D_{sf}, demonstrating that the microporous structure's complexity is significantly greater than that of the mesoporous structure.

Discussion

Relationship between the fractal dimension and shale mineral composition

There are many types of organic shale minerals, including quartz, feldspar, calcite, dolomite, clay minerals, pyrite, etc. There

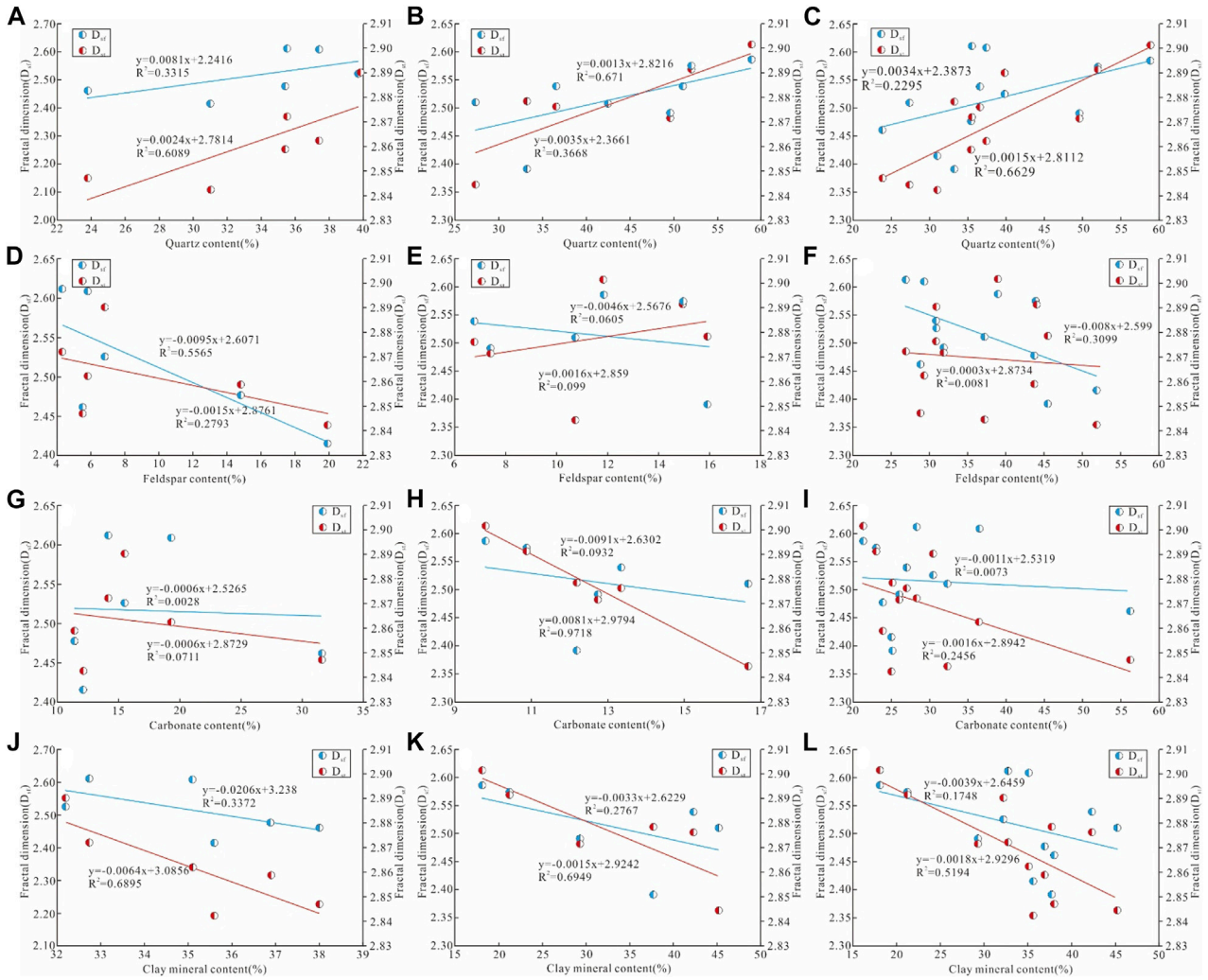

FIGURE 5
Correlation between the shale mineral composition and fractal dimension of the Longmaxi Formation in the Changning area. **(A–F)** is from ZK1, and **(G–L)** is from ZK2.

are certain differences in the content of mineral components in different regions, and their effects on the fractal dimension are also different (Kennedy et al., 2002; Liu et al., 2022b). Here, the relationship between the fractal dimension and quartz, feldspar (potassium feldspar + plagioclase), carbonate rock (calcite + dolomite), and clay minerals are analyzed (Figure 5).

There are positive correlations between the quartz content and fractal dimensions D_{sf} and D_{st}, among which the correlation coefficients of the quartz content in well ZK_1 and D_{sf} and D_{st} are 0.3315 and 0.6089, respectively (Figure 5A). The correlation coefficients of the quartz content in well ZK_2 and D_{sf} and D_{st} are 0.671 and 0.3668, respectively (Figure 5B), and the correlation coefficients of all samples with D_{sf} and D_{st} are 0.2295 and 0.6629, respectively (Figure 5C). Quartz is the most important brittle mineral, and its content is significant for the exploration and development of shale gas. The fractal dimension of shale and the quartz content in the Changning area are positively correlated, which is mainly related to the source of silica in the shale. The shale in Longmaxi Formation was deposited in a deep-water shelf environment. The deposition of a low siliceous biological framework formed a large number of biogenic quartzes, which increased the pores of organic matter, the number of micropores, and the fractal dimension of the shale. However, in sedimentary diagenesis, a small amount of terrigenous clastic siliceous materials inevitably enters, and the sorting and rounding degree is greater than the biogenic degree, reducing the complexity of the pores and the correlation coefficient.

The relationship between the feldspar content and fractal dimension in different wells is obviously different (Figures 5D–F). The feldspar content in well ZK_1 has a weak medium

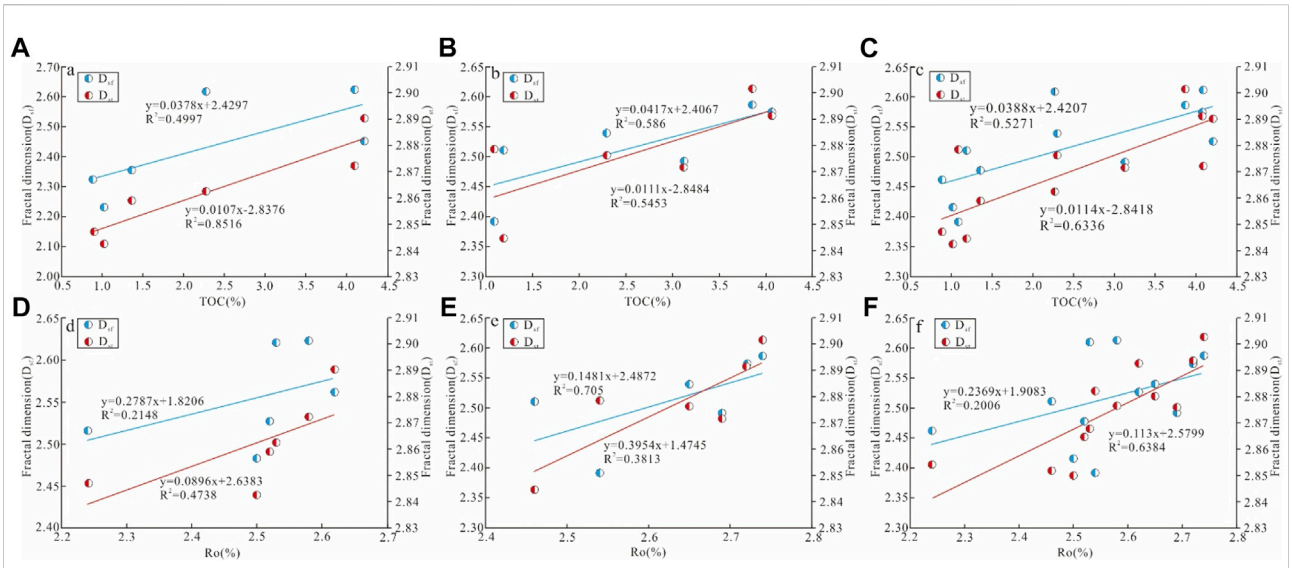

FIGURE 6
Correlation between the organic matter content and maturity and fractal dimension of the shale.

negative correlation with D_{sf} and D_{st}, with correlation coefficients of 0.5565 and 0.2793, respectively (Figure 5D). The feldspar after handling has a good sorting performance, which mainly plays a good role in the intergranular pores and dissolution pores, and the pore size formed is large, leading to the negative correlation between the feldspar content and fractal dimension. The feldspar content of well ZK_2 is weakly correlated with D_{sf} and D_{st}, with correlation coefficients of only 0.0605 and 0.099 (Figure 5E). The content of feldspar is very low (obviously lower than that of quartz), thus providing fewer pores. At the same time, feldspar mostly comes from terrigenous clasts, so it has little effect on the fractal dimension.

The correlation between the content of carbonate rock minerals and fractal dimension is generally very weak. The correlation coefficients of the carbonate rock content with D_{sf} and D_{st} in well ZK_1 are 0.0028 and 0.0711, respectively (Figure 5G), and those in well ZK_2 are 0.0932 and 0.9718, respectively (Figure 5H), while the correlation coefficients of all samples with D_{sf} and D_{st} are 0.0073, and 0.2456, respectively (Figure 5I). Some carbonate rocks exist in the form of cement, which fills and blocks the pores and reduces the connectivity of the pores. The negative correlation becomes stronger if the content is large and the filling is regular. In addition, carbonate rocks are soluble minerals, which often form large dissolution pores and have a weak contribution to the development of micropores. In general, the dual effect of carbonate rocks on pore development leads to the poor correlation between carbonate rocks and the microporous structure.

Compared with carbonate rock minerals, the negative correlation between clay minerals and the fractal dimension is obvious. The correlation coefficients between the clay mineral content of well ZK_1 and D_{sf} and D_{st} are 0.3372 and 0.6895 (Figure 5J), respectively. The correlation coefficients between the clay mineral content of well ZK2 and D_{sf} and D_{st} are 0.2767 and 0.6949, respectively (Figure 5K). In contrast, the correlation coefficients between all samples and D_{sf} and D_{st} are 0.1748, and 0.5194, respectively (Figure 5L). Clay minerals have strong plasticity. During long-term diagenesis, clay minerals are strongly compacted, which reduces the porosity of the reservoir, especially the number of micropores. In addition, the deformation and filling of clay minerals also reduce the connectivity of pores, thereby reducing the complexity of the pore structure.

Relationship between the fractal dimension and organic matter

Organic matter is the material basis for the formation of hydrocarbon gases. At the same time, it significantly impacts the pore structure of shale, mainly the content of TOC and the degree of thermal evolution (Ro). The former mainly affects the development of organic pores, while the latter affects the size and morphology of organic pores, thus affecting the fractal dimension of shale pores (Burruss et al., 1983; Gao et al., 2020; Sun et al., 2022).

The TOC content and fractal dimension show a good positive correlation. The correlation coefficients between the TOC content of well ZK_1 and D_{sf} and D_{st} are 0.4997 and 0.8516, respectively (Figure 6A), and the correlation coefficients between the TOC content of well ZK_2 and D_{sf} and D_{st} are 0.586 and

0.5453, respectively (Figure 6B), and the correlation coefficients between the TOC content of all samples and D_{sf} and D_{st} are 0.5271 and 0.6336, respectively (Figure 6C). With the increase in the TOC content, micropores, mesopores, and macropores increase, improving shale adsorption capacity for hydrocarbon gases. In contrast, with the increase in the TOC content, the increase in the fractal dimension D_{st} is more obvious (especially in well ZK_1), indicating that organic micro-mesopores are developed in the Changning area and that well ZK_1 is more developed than well ZK_2. With the increase in the organic carbon content, the number of micro-mesopores increases, and the pore structure tends to be more complex, which indicates that organic pores have a significant impact on the pore structure of shale.

The decomposition of kerogen or asphalt mainly forms the pores produced by organic matter during the ripening process, so the development of organic pores is related to the Ro of organic matter, which then affects the size of the fractal dimension. Ro and the fractal dimension are also positively correlated. The correlation coefficients of Ro in well ZK_1 with D_{sf} and D_{st} are 0.2148 and 0.4738, respectively (Figure 6D). The correlation coefficients of Ro in well ZK2 with D_{sf} and D_{st} are 0.705 and 0.3813, respectively (Figure 6E). The correlation coefficients of Ro in all samples with D_{sf} and D_{st} are 0.2006 and 0.6384, respectively (Figure 6F). The samples are high over the mature stage, the maturity increases, and the aromatization degree of organic matter intensifies, making the interior of the organic pores rougher. At the same time, the increase in organic matter will also reduce the support capacity. Under the overlying strata, the internal pore deformation of organic matter intensifies, reducing the connectivity between pores, increasing pore complexity, and increasing the fractal dimension.

Conclusion

In this paper, taking the organic-rich shale of Longmaxi formation in the Changning area as an example, based on whole rock X-ray diffraction, argon ion polishing electron microscopy observations, and low-temperature nitrogen adsorption-desorption experiments, the pore structure of shale was quantitatively characterized by using Frenkel Halsey Hill (FHH) model. The main conclusions are as follows:

1) The pores of the organic-rich shale in the Longmaxi Formation in the Changning area of southern Sichuan are mainly organic, intergranular pores, dissolution pores, and microfractures, with mainly micropores and mesopores. The pore morphology is ink bottle-type and semiclosed slit-type with good openness. Calculating the fractal dimension reveals that the shale has good dual fractal characteristics. The surface fractal dimension D_{sf} is between 2.3215 and 2.6117, the structural fractal dimension D_{st} is between 2.8424 and 2.9013, and the structural fractal dimension is greater than the surface fractal dimension.
2) The fractal dimension of the shale is affected by both inorganic minerals and organic matter. The fractal dimension has a good positive correlation with the quartz content but an obvious negative correlation with clay minerals. The correlation between the feldspar content and fractal dimension is either poor or nonexistent, and the relationship between carbonate minerals and the fractal dimension is a very weak negative correlation. The higher the total organic carbon content and thermal evolution degree are, the greater the number of micro-mesopores and the larger the pore fractal dimension.
3) The pore size distribution is wide for different types of shale. The pore structure of shale is quantitatively characterized by the low-temperature nitrogen adsorption-desorption experiment and the FHH model. The experimental methods and fractal calculation models are different for different pore sizes of shale. Therefore, the main research direction of shale pore quantitative characterization is to carry out the quantitative characterization of shale pores through high-pressure mercury injection, liquid nitrogen adsorption, carbon dioxide adsorption, and other experiments and to select different fractal dimensions models.

Data availability statement

The original contributions presented in the study are included in the article/supplementary material, further inquiries can be directed to the corresponding author.

Author contributions

HL, JZ, XM, SW, TZ, and SH contributed in writing, reviewing, and editing, datacuration, writing—original draft preparation; HG, XW, HA, QM, HL, CD, JW, and SZ contributed in formal analysis, validation, and reviewing.

Funding

This study was financially supported by the Open fund of Shale Gas Evaluation and Exploitation Key Laboratory of Sichuan Province (No. YSK2022002), Open fund of Natural Gas Geology Key Laboratory of Sichuan Province (No. 2021trqdz05) and the key R & D projects of the Deyang science and technology plan (NO. 2022SZ049 and 2021SZ002).

Acknowledgments

We thank all editors and reviewers for their helpful comments and suggestions.

Conflict of interest

Authors JZ, HL, XM, HG, XW, HA, QM, CD, JW, and SZ are employed by the PetroChina Southwest Oil and Gas Field Company.

The remaining authors declare that the research was conducted in the absence of any commercial or financial relationships that could be construed as a potential conflict of interest.

Publisher's note

All claims expressed in this article are solely those of the authors and do not necessarily represent those of their affiliated organizations, or those of the publisher, the editors and the reviewers. Any product that may be evaluated in this article, or claim that may be made by its manufacturer, is not guaranteed or endorsed by the publisher.

References

Ahmad, A. L., and Mustafa, N. N. N. (2006). Pore surface fractal analysis of palladium-alumina ceramic membrane using frenkel-Halsey-Hill (FHH) model. *J. Colloid Interface Sci.* 301 (2), 575–584. doi:10.1016/j.jcis.2006.05.041

Ambrose, R. J., Hartman, R. C., Campos, M. D., Akkutlu, I. K., and Sondergeld, C. (2010). New pore-scale considerations for shale gas in place calculations. *Soc. Pet. Eng.* 17 (1), 219–229. doi:10.2118/131772-PA

Ameen, M. S. (2016). Fracture modes in the silurian qusaiba shale play, northern Saudi Arabia and their geomechanical implications. *Mar. Pet. Geol.* 78, 312–355. doi:10.1016/j.marpetgeo.2016.07.013

Bu, H. L., Ju, Y. W., Tan, J. Q., Wang, G. C., and Li, X. S. (2015). Fractal characteristics of poresin non-marine shales from the huainan coalfield, eastern China. *J. Nat. Gas. Sci. Eng.* 24, 166–177. doi:10.1016/j.jngse.2015.03.021

Burruss, R. C., Cerone, K. R., and Harris, P. M. (1983). Fluid inclusion petrography and tectonic-burial history of the A1 Ali No.2 well:evidence for the timing of diagenesis and oil migration, northern Oman Foredeep. *Geology* 11, 567

Chang, J. Q., Fan, X. D., Jiang, Z. X., Wang, X. M., Chen, L., Li, J. T., et al. (2022). Differential impact of clay minerals and organic matter on pore structure and its fractal characteristics of marine and continental shales in China. *Appl. Clay Sci.* 216, 106334. doi:10.1016/j.clay.2021.106334

Cheng, G. X., Jiang, B., Li, M., Li, F. L., and Zhu, M. (2021). Structural evolution of southern sichuan basin (South China) and its control effects on tectonic fracture distribution in longmaxi shale. *J. Struct. Geol.* 153, 104465. doi:10.1016/j.jsg.2021.104465

Fan, C. H., Li, H., Qin, Q. R., He, S., and Zhong, C. (2020a). Geological conditions and exploration potential of shale gas reservoir in wufeng and longmaxi formation of southeastern sichuan basin, China. *J. Pet. Sci. Eng.* 191, 107138. doi:10.1016/j.petrol.2020.107138

Fan, C. H., Li, H., Qin, Q. R., Shang, L., Yuan, Y. F., and Li, Z. (2020c). Formation mechanisms and distribution of weathered volcanic reservoirs: A case study of the carboniferous volcanic rocks in northwest junggar basin, China. *Energy Sci. Eng.* 8, 2841–2858. doi:10.1002/ese3.702

Fan, C. H., Li, H., Zhao, S. X., Qin, Q. R., Fan, Y., Wu, J. F., et al. (2020b). Formation stages and evolution patterns of structural fractures in marine shale: Case study of the lower silurian Longmaxi formation in the changning area of the southern Sichuan Basin, China. *Energy fuels.* 34 (8), 9524–9539. doi:10.1021/acs.energyfuels.0c01748

Fan, C. H., Xie, H. B., Li, H., Zhao, S. X., Shi, X. C., Liu, J. F., et al. (2022). Complicated fault characterization and its influence on shale gas preservation in the southern margin of the Sichuan Basin, China. *China. Lithosphere* 2022, 8035106. doi:10.2113/2022/8035106

Feng, Z. Q., Liu, D., Huang, S, P., Wu, W., Dong, D. Z., Peng, W. L., et al. (2016). Carbon isotopic composition of shale gas in the silurian Longmaxi formation of the changning area, Sichuan Basin. *Petroleum Explor. Dev.* 43 (5), 769–777. doi:10.1016/S1876-3804(16)30092-1

Gao, F. Q. (2019). Use of numerical modeling for analyzing rock mechanic problems in underground coal mine practices. *J. Min. Strata Control Eng.* 1 (1), 013004. doi:10.13532/j.jmsce.cn10-1638/td.2019.02.009

Gao, Z., Fan, Y., Xuan, Q., and Zheng, G. (2020). A review of shale pore structure evolution characteristics with increasing thermal maturities. *Adv. Geo-Energy Res.* 4 (3), 247–259. doi:10.46690/ager.2020.03.03

He, D. F., Liu, R. Q., Huang, H, Y., Wang, X. S., Jiang, H., and Zhang, W. K. (2019). Tectonic and geological setting of the earthquake hazards in the Changning shale gas development zone, Sichuan Basin, SW China. *Petroleum Explor. Dev.* 46 (5), 1051–1064. doi:10.1016/S1876-3804(19)60262-4

He, S., Li, H., Qin, Q. R., and Long, S. X. (2021). Influence of mineral compositions on shale pore development of Longmaxi Formation in the Dingshan area, southeastern Sichuan Basin, China. *Energy fuels.* 35 (13), 10551–10561. doi:10.1021/acs.energyfuels.1c01026

He, S., Qin, Q. R., Li, H., and Wang, S. L. (2022b). Deformation differences in complex structural areas in the southern Sichuan Basin and its influence on shale gas preservation: A case study of changning and luzhou areas. *Front. Earth Sci. (Lausanne).* 9, 818155. doi:10.3389/feart.2021.818534

He, S., Qin, Q. R., Li, H., and Zhao, S. X. (2022a). Geological characteristics of deep shale gas in the silurian Longmaxi formation in the southern Sichuan Basin, China. *Front. Earth Sci. (Lausanne).* 9, 818543. doi:10.3389/feart.2021.818155

Jin, Z. J., Nie, H. K., Liu, Q. Y., Zhao, J. H., and Jiang, T. (2018). Source and seal coupling mechanism for shale gas enrichment in upper ordovician wufeng formation - lower silurian longmaxi formation in sichuan basin and its periphery. *Mar. Pet. Geol.* 97, 78–93. doi:10.1016/j.marpetgeo.2018.06.009

Kennedy, M. J., Pevear, D. R., and Hill, R. J. (2002). Mineral surface control of organic carbon in black shale. *Science* 295 (5555), 657–660. doi:10.1126/science.1066611

Li, H. (2021). Quantitative prediction of complex tectonic fractures in the tight sandstone reservoirs: A fractal method. *Arab. J. Geosci.* 14, 1986. doi:10.1007/s12517-021-08344-0

Li, H., Qin, Q. R., Zhang, B. J., Ge, X. Y., Hu, X., Fan, C. H., et al. (2020). Tectonic fracture formation and distribution in ultradeep marine carbonate gas reservoirs: A case study of the maokou formation in the jiulongshan gas field, Sichuan Basin, southwest China. *Energy Fuels.* 34 (11), 14132–14146. doi:10.1021/acs.energyfuels.0c03327

Li, H. (2022). Research progress on evaluation methods and factors influencing shale brittleness: A review. *Energy Rep.* 8, 4344–4358. doi:10.1016/j.egyr.2022.03.120

Li, H., Tang, H. M., Qin, Q. R., Fan, C. H., Han, S., Yang, C., et al. (2018). Reservoir characteristics and hydrocarbon accumulation of Carboniferous volcanic weathered crust of Zhongguai high area in the Western Junggar Basin, China. *J. Cent. South Univ.* 25 (11), 2785–2801. doi:10.1007/s11771-018-3953-y

Li, H., Tang, H. M., Qin, Q. R., Wang, Q., and Zhong, C. (2019c). Effectiveness evaluation of natural fractures in Xujiahe Formation of Yuanba area, Sichuan basin, China. *Arab. J. Geosci.* 12 (6), 194. doi:10.1007/s12517-019-4292-5

Li, H., Tang, H. M., Qin, Q. R., Zhou, J. L., Qin, Z. J., Fan, C. H., et al. (2019b). Characteristics, formation periods and genetic mechanisms of tectonic fractures in the tight gas sandstones reservoir: A case study of xujiahe formation in YB area, Sichuan Basin, China. *J. Petroleum Sci. Eng.* 178, 723–735. doi:10.1016/j.petrol.2019.04.007

Li, H., Tang, H. M., and Zheng, M. J. (2019a). Micropore structural heterogeneity of siliceous shale reservoir of the Longmaxi Formation in the southern Sichuan Basin, China. *Minerals* 9, 548. doi:10.3390/min9090548

Li, H. T., Peng, R., Du, W. S., Li, X. P., and Zhang, N. B. (2021a). Experimental study on structural sensitivity and intervention mechanism of mechanical behavior of coal samples. *J. Min. Strata Control Eng.* 3 (4), 043012. doi:10.13532/j.jmsce.cn10-1638/td.20210820.001

Li, H., Wang, Q., Qin, Q. R., and Ge, X. Y. (2021b). Characteristics of natural fractures in an ultradeep marine carbonate gas reservoir and their impact on the reservoir: A case study of the maokou formation of the jls structure in the Sichuan Basin, China. *Energy fuels.* 35 (16), 13098–13108. doi:10.1021/acs.energyfuels.1c01581

Li, J. J., Qin, Q. R., Li, H., and Wan, Y. F. (2022c). Numerical simulation of the stress field and fault sealing of complex fault combinations in Changning area, Southern Sichuan Basin, China. *Energy Sci. Eng.* 10, 278–291. doi:10.1002/ese3.1044

Li, J. J., Yin, J. X., Zhang, Y. N., Lu, S. F., Wang, W. M., Li, J. B., et al. (2015). A comparison of experimental methods for describing shale pore features - a case study in the Bohai Bay Basin of eastern China. *Int. J. Coal Geol.* 152, 39–49. doi:10.1016/j.coal.2015.10.009

Li, J., Li, H., Xu, J. L., Wu, Y. J., and Gao, Z. (2022a). Effects of fracture formation stage on shale gas preservation conditions and enrichment in complex structural areas in the southern sichuan basin, china. *Front. Earth Sci. (Lausanne).* 9, 823855. doi:10.3389/feart.2022.921988

Li, J., Li, H., Yang, C., Wu, Y. J., Gao, Z., and Jiang, S. L. (2022b). Geological characteristics and controlling factors of deep shale gas enrichment of the Wufeng-Longmaxi Formation in the southern Sichuan Basin, China. *Lithosphere* 2022, 4737801. doi:10.2113/2022/4737801

Liu, J. S., Ding, W. L., Gu, Y., Xiao, Z. K., Dai, J. S., Dai, P., et al. (2018b). Methodology for predicting reservoir breakdown pressure and fracture opening pressure in low-permeability reservoirs based on an *in situ* stress simulation. *Eng. Geol.* 246, 222–232. doi:10.1016/j.enggeo.2018.09.010

Liu, J. S., Yang, H. M., Bai, J. P., Wu, K. Y., Zhang, G. J., Liu, Y., et al. (2021). Numerical simulation to determine the fracture aperture in a typical basin of China. *Fuel* 283, 118952. doi:10.1016/j.fuel.2020.118952

Liu, J. S., Yang, H. M., Wu, X. F., and Liu, Y. (2020). The *in situ* stress field and microscale controlling factors in the ordos basin, central china. *Int. J. Rock Mech. Min. Sci. (1997).* 135, 104482. doi:10.1016/j.ijrmms.2020.104482

Liu, J. S., Yang, H. M., Xu, K., Wang, Z. M., Liu, X. Y., Cui, L. J., et al. (2022a). Genetic mechanism of transfer zones in rift basins: Insights from geomechanical models. *GSA Bull.* doi:10.1130/B36151.1

Liu, J. S., Zhang, G. J., Bai, J. P., Ding, W. L., Yang, H. M., and Liu, Y. (2022b). Quantitative prediction of the drilling azimuth of horizontal wells in fractured tight sandstone based on reservoir geomechanics in the Ordos Basin, central China. *Mar. Pet. Geol.* 136, 105439. doi:10.1016/j.marpetgeo.2021.105439

Liu, J., Yao, Y. B., Liu, D. M., Cai, Y. D., and Cai, J. C. (2018a). Comparison of pore fractal characteristics between marine and continental shales. *Fractals* 26 (2), 1840016. doi:10.1142/s0218348x18400169

Liu, K. Q., Ostadhassan, M., and Kong, L. Y. (2019). Fractal and multifractal characteristics of pore throats in the bakken shale. *Transp. Porous Media* 126 (3), 579–598. doi:10.1007/s11242-018-1130-2

Ma, X. H., Wang, H. Y., Zhou, S. W., Shi, Z. S., and Zhang, L. F. (2021). Deep shale gas in China: Geological characteristics and development strategies. *Energy Rep.* 7, 1903–1914. doi:10.1016/j.egyr.2021.03.043

Ma, Y. Z., Wang, M., Zhao, X. Z., Dai, X. G., and He, Y. (2022). Study of the microstructural characteristics of low-rank coal under different degassing pressures. *Energies* 15 (10), 3691. doi:10.3390/en15103691

Mandelbrot, B. B. (1978). Fractal objects. *Recherche* 9 (85), 5.

Mandelbrot, B. B. (1984). Fractals in physics - squig clusters, diffusions, fractal measures, and the unicity of fractal dimensionality. *J. Stat. Phys.* 34 (5-6), 895–930. doi:10.1007/BF01009448

Mandelbrot, B. B. (1985). Self-affine fractals and fractal dimension. *Phys. Scr.* 32 (4), 257–260. doi:10.1088/0031-8949/32/4/001

Pan, S. X., Zha, M., Gao, C. H., Qu, J. X., and Ding, X. J. (2021). Pore structure and fractal characteristics of organic-rich lacustrine shales of the kongdian formation, cangdong sag, bohai bay basin. *Front. Earth Sci.* 9, 760538. doi:10.3389/feart.2021.760583

Qiu, Z., Song, D. J., Zhang, L. F., Zhang, Q., Zhao, Q., Wang, Y. M., et al. (2021). The geochemical and pore characteristics of a typical marine-continental transitional gas shale: A case study of the permian shanxi formation on the eastern margin of the ordos basin. *Energy Rep.* 7, 3726–3736. doi:10.1016/j.egyr.2021.06.056

Shan, S. C., Wu, Y. Z., Fu, Y. K., and Zhou, P. H. (2021). Shear mechanical properties of anchored rock mass under impact load. *J. Min. Strata Control Eng.* 3 (4), 043034. doi:10.13532/j.jmsce.cn10-1638/td.20211014.001

Song, J. F., Lu, C. P., Li, Z. W., Ou, Y. G. C., Cao, X. M., and Zhou, F. L. (2021). Characteristics of stress distribution and microseismic activity in rock parting occurrence area. *J. Min. Strata Control Eng.* 3 (4), 043518. doi:10.13532/j.jmsce.cn10-1638/td.20210607.002

Sun, Y., Ju, Y., Zhou, W., Qiao, P., Tao, L., and Xiao, L. (2022). Nanoscale pore and crack evolution in shear thin layers of shales and the shale gas reservoir effect. *Adv. Geo-Energy Res.* 6 (3), 221–229. doi:10.46690/ager.2022.03.05

Tang, L., Song, Y., Jiang, Z. X., Jiang, S., and Li, Q. W. (2019). Pore structure and fractal characteristics of distinct thermally mature shales. *Energy fuels.* 33 (6), 5116–5128. doi:10.1021/acs.energyfuels.9b00885

Tang, X., Zheng, F. Z., Liang, G. D., Ma, Z. J., Zhang, J. Z., Wang, Y. F., et al. (2022). Fractal characterization of pore structure of cambrian niutitang shale in northern Guizhou Province, southwestern China. *Earth Sci. Front. Online*. doi:10.13745/j.esf.sf.2022.5.36

Wang, B., Zhou, F. J., Zhou, H., Ge, H., and Li, L. Z. (2021). Characteristics of the fracture geometry and the injection pressure response during near-wellbore diverting fracturing. *Energy Rep.* 7, 491–501. doi:10.1016/j.egyr.2020.12.039

Wang, J., and Wang, X. L. (2021). Seepage characteristic and fracture development of protected seam caused by mining protecting strata. *J. Min. Strata Control Eng.* 3 (3), 033511. doi:10.13532/j.jmsce.cn10-1638/td.20201215.001

Wang, R. Y., Hu, Z. Q., Long, S. X., Liu, G. X., Zhao, J. H., Dong, L., et al. (2019). Differential characteristics of the Upper Ordovician-Lower Silurian Wufeng-Longmaxi shale reservoir and its implications for exploration and development of shale gas in/around the Sichuan Basin. *Acta Geol. Sin.* 93 (3), 520–535. doi:10.1111/1755-6724.13875

Wang, R. Y., Hu, Z. Q., Sun, C. X., Liu, Z. B., Zhang, C. C., Gao, B., et al. (2018). Comparative analysis of shale reservoir characteristics in the wufeng-longmaxi (O_3w-S_1l) and niutitang ($\epsilon_1 n$) formations: A case study of wells JY1 and TX1 in the southeastern sichuan basin and its neighboring areas, southwestern China. *Interpretation* 6 (4), SN31–SN45. doi:10.1190/int-2018-0024.1

Wang, R. Y., Nie, H. K., Hu, Z. Q., Liu, G. X., Xi, B. B., and Liu, W. X. (2020). Controlling effect of pressure evolution on shale gas reservoirs: A case study of the Wufeng-Longmaxi formation in the Sichuan Basin. *Nat. Gas. Ind.* 40 (10), 1–11. doi:10.3787/j.issn.1000-0976.2020.10.001

Wang, S. L., Li, H., Lin, L. F., and Yin, S. (2022). Development characteristics and finite element simulation of fractures in tight oil sandstone reservoirs of Yanchang Formation in Western Ordos Basin. *Front. Earth Sci. (Lausanne).* 9, 823855. doi:10.3389/feart.2021.823855

Wei, D., Gao, Z. Q., Zhang, C., Fan, T. L., Karubandika, G. M., and Meng, M. M. (2019). Pore characteristics of the carbonate shoal from fractal perspective. *J. Pet. Sci. Eng.* 174, 1249–1260. doi:10.1016/j.petrol.2018.11.059

Wu, J. F., Zhao, S. X., Fan, C. H., Xia, Z. Q., Ji, C. H., Zhang, C. L., et al. (2021). Fracture characteristics of the Longmaxi Formation shale and its relationship with gas-bearing properties in Changning area, southern Sichuan. *Acta Pet. Sin.* 42 (4), 428–446. doi:10.7623/syxb202104002

Xi, Z. D., Tang, S. H., Wang, J., Yi, J. J., Guo, Y. Y., and Wang, K. F. (2018). Pore structure and fractal characteristics of niutitang shale from China. *Minerals* 8 (4), 163. doi:10.3390/min8040163

Xu, Q. L., Liu, B., Ma, Y. S., Song, X. M., Wang, Y. J., and Chen, Z. X. (2017). Geological and geochemical characterization of lacustrineshale: A case study of the jurassic da'anzhai membershalein the central Sichuan Basin, southwest China. *J. Nat. Gas. Sci. Eng.* 47, 124–139. doi:10.1016/j.jngse.2017.09.008

Yang, C., Zhang, J. C., Wang, X. Z., Tang, X., Chen, Y. C., Jiang, L., et al. (2017). Nanoscale pore structure and fractal characteristics of a marine-continental transitional shale: A case study from the lower permian shanxi shale in the southeastern ordos basin, China. *Mar. Pet. Geol.* 88, 54–68. doi:10.1016/j.marpetgeo.2017.07.021

Yang, Y. Y., Zhang, J. C., Xu, L. F., Li, P., Liu, Y., and Dang, W. (2022). Pore structure and fractal characteristics of deep shale: A case study from permian shanxi formation shale, from the ordos basin. *ACS Omega* 7 (11), 9229–9243. doi:10.1021/acsomega.1c05779

Zhan, H. L., Yang, Y. Q., Zhang, Y., Miao, X. Y., Zhao, K., and Yue, W. Z. (2021). Terahertz for the detection of the oil bearing characteristics of shale. *Energy Rep.* 7, 5162–5167. doi:10.1016/j.egyr.2021.08.109

Zhang, P., Huang, Y. Q., Zhang, J. C., Liu, H. Y., and Yang, J. W. (2018). Fractal characteristics of the Longtan formation transitional shale in northwest GuizhouJ. *China Coal Soc.* 43 (6), 1580–1588. doi:10.13225/j.cnki.jccs.2018.4046